

## Modelling of tungsten erosion, transport and deposition in fusion devices

A. Kirschner<sup>1</sup>, S. Brezinsek<sup>1</sup>, D. Tskhakaya<sup>2</sup>, D. Borodin<sup>1</sup>, J. Romazanov<sup>1</sup>, A. Eksaeva<sup>1</sup>,  
R. Ding<sup>3</sup>, Ch. Linsmeier<sup>1</sup>, and JET contributors

*EUROfusion Consortium JET, Culham Science Centre Abingdon, OX14 3DB, UK*

<sup>1</sup> *Forschungszentrum Jülich GmbH, Institut für Energie- und Klimaforschung – Plasmaphysik, Partner of the Trilateral Euregio Cluster (TEC), 52425 Jülich, Germany*

<sup>2</sup> *Fusion@ÖAW, Department of Mathematics, University of Innsbruck, A-6020, Innsbruck, Austria*

<sup>3</sup> *Institute of Plasma Physics, ASIPP, Hefei, Anhui 230031, P.R. China*

### Introduction

The erosion of wall material in fusion devices is a critical issue due to wall components lifetime, plasma contamination and fuel retention caused by co-deposition of eroded material. Tungsten (W) erosion is studied in JET-ILW, presently the only tokamak with an ITER-like wall, i.e. beryllium (Be) main wall and tungsten divertor. Understanding of erosion, impurity transport and deposition is gained by dedicated experiments in combination with modelling. For this, ERO [1] modelling has been done in the past for specific JET-ILW pulses to reproduce W erosion in the outer divertor by analysing spatially and temporally resolved WI emission [2]. The contributions of inter- and intra-ELM phases to the overall erosion and the role of redeposition could be clarified.

The present contribution studies in more detail the dynamics of erosion and deposition. The originally pure W divertor surface is intermixed with Be originating from main wall erosion. By means of a simple material mixing model, which dynamically calculates the surface concentrations of W and Be within an interaction layer, the time evolution of the surface composition is modelled with ERO. The focus is on the dynamics of the outer divertor tile 5 of JET-ILW for inter- and intra-ELM conditions. Also, first results of modelling consecutive inter- and intra-ELM phases is presented.

### Dynamic erosion / deposition of the outer divertor in JET-ILW

Inter-ELM plasma parameters at the strike point (SP) of  $T_{e,i} = 35$  eV and  $n_e = 6E19$  m<sup>-3</sup>, corresponding to the C30C campaign, are applied [3]. Using exponential decay lengths perpendicular to the separatrix towards the scrape-off layer (SOL) and the private flux region (PFR) deliver 2D distributions of the plasma parameters within the poloidal plane, see also [2]. The Be influx into the outer divertor is assumed to be 0.5% relative to the deuterium ion flux

[2]. Figure 1a shows the modelled steady state profile of W surface concentration along tile 5. Whereas in the deep PFR the W concentration is still near to 1, there is an area within the PFR near to the SP with very small W surface concentrations. The dynamic evolution of the W surface concentration at specific locations is shown in figure 1b. The initially pure W surface is mixed with Be, leading to steady state values after certain exposure time. For the simulations a time step  $\Delta t = 0.1$ s and an interaction layer thickness of  $\lambda_{int} = 40$  nm is used. It has to be noted that the time evolution scales linearly with  $\lambda_{int}$ , however, the steady state concentrations are independent of  $\lambda_{int}$ . Also, similar time scales as resulting from surface mixing models based on binary collision approximation codes like SDTrimSP, are obtained when  $\lambda_{int}$  resembles typical penetration depths of incoming particles [4].

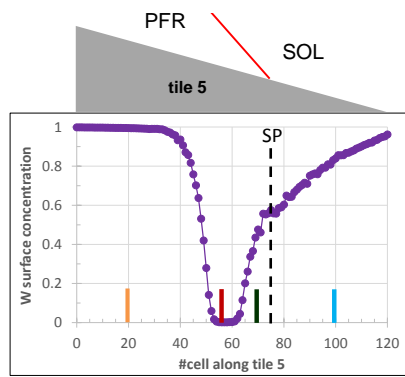


**Fig. 1a** Modelled W surface concentration along tile 5 for inter-ELM conditions.

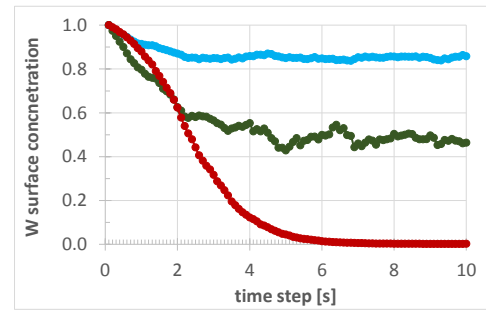


**Fig. 1b** Modelled time evolution of W surface concentrations at various locations on tile 5 (colours correspond to locations as marked in fig. 1a).

The time evolution of W gross erosion is presented in figure 2a showing, after an initial increase, constant steady state gross erosion rates in the SOL and the PFR near the SP. The initial increase is due to the fact that erosion of eroded particles is calculated in the subsequent time step of the simulation. Going deeper into the PFR to locations of very small steady state W surface concentration leads to very small W gross erosion as it is proportional to the surface concentration. Figure 2b shows the time evolution of the Be resource (the accumulated number of deposited Be atoms) at various locations. It is seen that within the SOL and at locations inside the PFR near to the SP constant Be resource values are obtained which means that the incoming Be flux equals the outgoing one. Deeper inside the PFR with smaller  $T_e$  and therefore reduced erosion, the Be resource increases linearly and thus a net Be layer is built up at these locations. The overall resulting net erosion / deposition profiles of Be and W along tile 5 for inter-ELM conditions are summarised in figure 3. For Be a net deposition zone is seen within the PFR showing a peak deposition next to the SP. Going further towards the SOL leads to a zone of balanced Be erosion / deposition and thus no net Be layer formation.

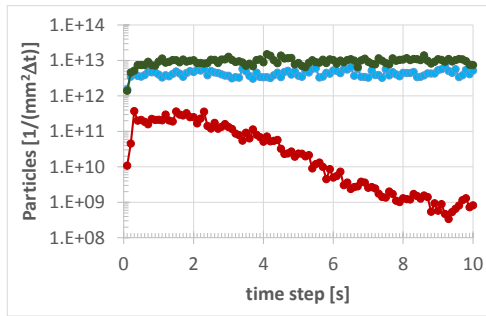


**Fig. 2a** Modelled time evolution of W gross erosion at various locations on tile 5 (colours correspond to locations as marked in fig. 1a).

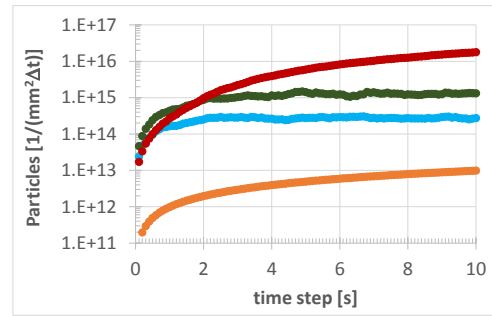


**Fig. 2b** Modelled time evolution of Be resource at various locations on tile 5 (colours correspond to locations as marked in fig. 1a).

In case of W three zones can be identified. Within the deep PFR the small electron temperatures result in too low impact energies and thus no significant W sputtering is observed. Going further towards the SP shows net W deposition, with – similar to Be – peaked deposition near to the SP. Near the SP and within the whole SOL net W erosion is simulated. The peaked deposition of Be and W within the PFR near to the SP is a result of the  $E \times B$  drift, which transports particles eroded in the SOL towards the PFR. These net Be and W deposition peaks disappear in simulations with reversed B field (not shown here).

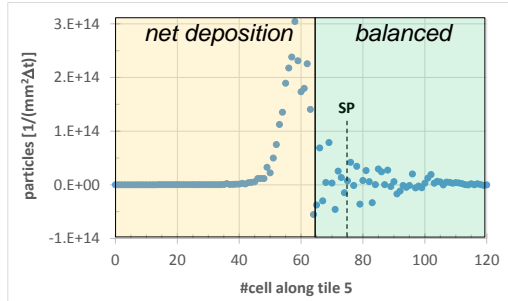


**Fig. 3** Simulated steady state net erosion / deposition profiles of Be (left) and W (right) along tile 5 for inter-ELM conditions.

Simulations for ELM conditions have been performed assuming the same electron temperature as for inter-ELM conditions, but higher electron density ( $1E20 \text{ m}^{-3}$  at the SP) and large ion impact energy (1 keV for deuterium ions). According to the conditions of C30C an ELM frequency of 30 Hz and ELM duration of  $500 \mu\text{s}$  has been used. As for the inter-ELM phases a Be influx of 0.5% relative to the deuterium ion flux is assumed. Figure 4 shows the resulting steady state net erosion / deposition profiles including the contributions of ELM and inter-ELM phases and the sum of both. The rates represent the erosion within 1s considering the frequency and duration of the ELMs. In case of beryllium the erosion and deposition is dominated by the inter-ELM phases. The electron temperature between ELMs is large enough for significant Be sputtering and although the Be flux is larger during the ELMs, the overall contribution from the inter-ELM phases within 1s is greater due to the small ELM duration and frequency. This is

different for W, as the erosion of W due to ELMs is much larger than in-between ELMs. Still, the inter-ELM phases have significant contributions, however, within 1s the net erosion from ELMs is about 2.5 times larger than the one from the inter-ELM phases.

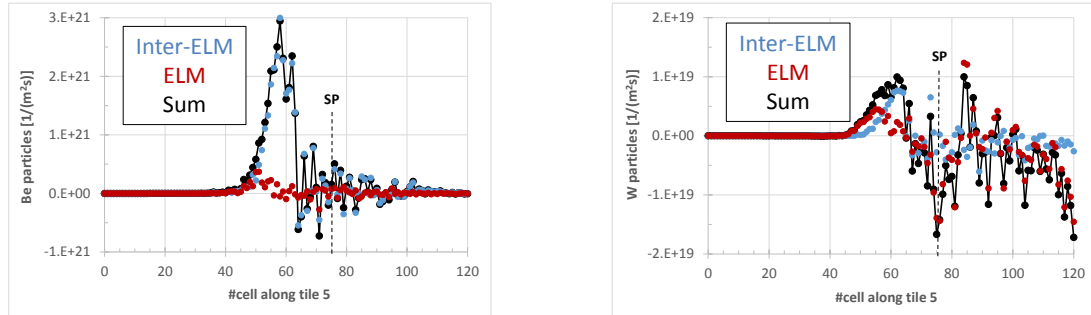


**Fig. 4** Simulated steady state net erosion / deposition profiles of Be (left) and W (right) along tile 5 for inter-ELM, ELM conditions and the sum of both within 1s.

### Simulations of consecutive inter-ELM and ELM phases

So far the inter-ELM and ELM phases have been treated separately. In the following first simulation results are shown for an ERO run with subsequent inter-ELM and ELM conditions. The time constant  $\Delta t$  for the simulation steps has to be reduced significantly to resolve the different phases:  $\Delta t_{\text{inter-ELM}} = 3280\mu\text{s}$  and  $\Delta t_{\text{ELM}} = 50\mu\text{s}$  resulting in 11 time steps per inter-ELM phase and 10 steps per ELM phase. Figure 5 shows the resulting surface-integrated (over tile 5) gross W erosion in dependent on the time step and the resulting net erosion / deposition profile along tile 5 together with the simulation with only inter-ELM conditions after 5 inter-ELM phases. The results suggest that in steady state both simulations (consecutive inter- and intra-ELM phases vs. only inter-ELM phases) will lead to almost the same profile.

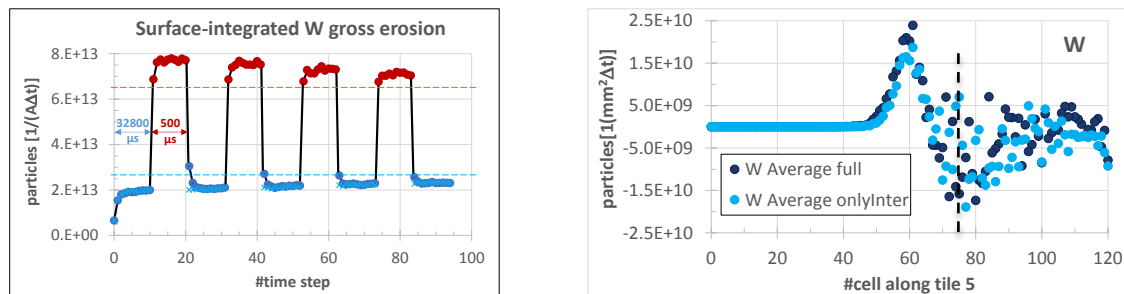


**Fig. 5** **Left:** Surface-integrated gross W erosion. The dotted lines indicate the steady state erosion value for only inter-ELM (turquoise) and only ELM (orange) simulations. **Right:** W net erosion / deposition profile along tile 5 for full consecutive simulation and for only inter-ELM condition (both averaged over last 11 steps). Steady state is not yet reached.

### References

- [1] A. Kirschner et al., Nucl. Fus. Vol. 40, No. 5 (2000) 989
- [2] A. Kirschner et al., Nuclear Mat. Energy 18 (2019) 239
- [3] S. Brezinsek et al., Nucl. Fus. (2019) <https://doi.org/10.1088/1741-4326/ab2aef>
- [4] S. Droste, Berichte des Forschungszentrums Jülich, JüL-4253 (2007)